J Mol Model (2012) 18:3617–3625
DOI 10.1007/s00894-012-1370-y

ORIGINAL PAPER

Toward a better understanding of the interaction between TGF-β family members and their ALK receptors

Valentina Romano · Domenico Raimondo · Luisa Calvanese · Gabriella D'Auria · Anna Tramontano · Lucia Falcigno

Received: 22 November 2011 / Accepted: 25 January 2012 / Published online: 22 February 2012

Abstract Transforming growth factor-beta (TGF-β) proteins are a family of structurally related extracellular proteins that trigger their signaling functions through interaction with the extracellular domains of their cognate serine/threonine kinase receptors. The specificity of TGF-β/receptor binding is complex and gives rise to multiple functional roles. Additionally, it is not completely understood at the atomic level. Here, we use the most reliable computational methods currently available to study systems involving activin-like kinase (ALK) receptors ALK4 and ALK7 and their multiple TGF-β ligands. We built models for all these proteins and their complexes for which experimental structures are not available. By analyzing the surfaces of interaction in six different TGF-β/ALK complexes we could infer which are the structural distinctive features of the ligand-receptor binding mode. Furthermore, this study allowed us to rationalize why binding of the growth factors GDF3 and Nodal to the ALK4 receptor requires the Cripto co-factor, whilst binding to the ALK7 receptor does not.

Keywords Comparative modeling · TGF-β protein · ALK receptor · Protein–protein docking

Abbreviations

ActRII	Activin type II receptor
ACVR1	Activin A type 1 receptor
ALK	Activin receptor-like kinase
ASA	Accessible surface area
BMP	Bone morphogenetic protein
BMPR1A	Bone morphogenetic protein type 1A receptor or ALK3
BMPRII	Bone morphogenetic protein type II receptor
BSA	Buried surface area
ECD	Extracellular domain
GDF	Growth/differentiation factor
MISRII	Mullerian inhibitor substance type II receptor
PP	Pair potential
TGF-β	Transforming growth factor-beta
TGFBRI	Type I TGF-β receptor or ALK5
TGF-βRII	Type II TGF-β receptor

Introduction

Growth factors belonging to the TGF-β superfamily control several cellular processes [1, 2], from development [3, 4] to proliferation [5–7] and differentiation [8, 9], from motility [10] and adhesion [11] to neuronal growth [12, 13] and bone morphogenesis [14], to cite a few. Many cellular pathways of TGF-β are also involved in pathological processes, such as carcinogenesis [15, 16], vascular disorders [17] and other

Valentina Romano and Domenico Raimondo contributed equally to this work.

Electronic supplementary material The online version of this article (doi:10.1007/s00894-012-1370-y) contains supplementary material, which is available to authorized users.

V. Romano · L. Calvanese · G. D'Auria · L. Falcigno
Department of Chemical Sciences,
Federico II University of Naples,
Via Cinthia 45,
80126 Naples, Italy

D. Raimondo · A. Tramontano
Department of Physics, Sapienza University of Rome,
P.le A. Moro, 5,
00185 Rome, Italy

G. D'Auria · L. Falcigno (✉)
Institute of Biostructures and Bioimaging—CNR,
Via Mezzocannone 16,
80134 Naples, Italy
e-mail: falcigno@unina.it

human diseases [18]. All members of this superfamily are synthesized as precursors that, after processing, give raise to a mature protein of about 100 amino acids. Mature TGF-β proteins act as homo or hetero dimers [1, 19]. From a structural point of view, all monomers share a common topology, the "cysteine-knot cytokines" fold comprising a conserved "cysteine-knot" motif [20–22], important for structural integrity, four pairs of antiparallel β-strands and an α-helix (α3) (see Supplementary Material Fig. S1). This protein fold resembles a hand, where the β-sheet mimics the fingers and the α-helix, α3, the wrist [1]. All these proteins exert their functions through binding to the extracellular domains (ECDs) of their cognate serine/threonine kinase receptors of type I and II [23]. Both receptor types are transmembrane glycoproteins of about 500 amino acids organized in an extracellular N-terminal domain, a transmembrane region, and an intracellular C-terminal domain with a kinase activity [2, 19]. The ECDs bind TGF-β ligands and share the "snake toxin-like" fold characterized by a conserved scaffold of disulfide bonds and consisting of three pairs of antiparallel β-strands, namely fingers 1 (formed by strands β1 and β2), 2 (formed by strands β3 and β4) and 3 (formed by strand β5 and strand β6), linked by loops [24]. The loop between fingers 2 and 3, named loop 23, belongs to the region involved in TGF-β binding for both receptors [25] (see Supplementary Material Fig. S1). In general, the TGF-β proteins bind as dimers to a complex formed by two type I and two type II receptors and form an heteromeric complex on the cell membrane [1, 26]. In such a complex, the TGF-β ligand binds to type I receptor through its "wrist epitope" corresponding to the wrist helix α3, the pre-helix loop of one monomer and the concave finger surface of the other monomer, and binds to type II receptor through the convex finger surface, the so called "knuckle epitope" of each monomer [1, 27, 28]. Nearly 40 TGF-β proteins have been identified in the human genome. They interact with seven members of the type I family of receptors (called ALK followed by a number ranging from 1 to 7) and five from the type II family (TGF-βRII, BMPRII, ActRIIA, ActRIIB, MISRII) [23, 27, 29]. Different TGF-βs show different affinity for their cognate receptors. Furthermore, their signal transduction activity is regulated by antagonists, modulators and co-receptors (e.g., Follistatin or Cripto) [2].

The structural basis for the specificity and affinity of the TGF-β factors and their receptors is not well understood. Some ligands seem to be able to exert similar, although not identical, functions by binding to different receptors, in some cases requiring the presence of additional co-receptors.

An interesting case is represented by the activin receptor-like kinase (ALK) type I receptors ALK4 and ALK7, also known as ACVR1B and ACVR1C, respectively. Both receptors bind the GDF3, Nodal and GDF11 factors [30–34]. Interestingly, however, ALK4 can bind GDF3 and Nodal only in the presence of the Cripto co-receptor [32, 33] , which is not necessary for GDF11-ALK4 binding [31]. ALK4 and ALK7 also bind GDF8 [35], (J. Knopf and J. Seehra, 2008; PATENT No: US 7,456,149 B2). A scheme of the known interactions between the factors and their cognate receptors is shown in Table 1.

GDF3 is expressed in the adipose tissue, where it regulates several functions such as fat accumulation and energy balance [30]; however, it is also present at elevated levels in pluripotent embryonic cells but its role in this compartment is unclear [36]. Nodal is thought to be the physiological ligand of ALK7 [7] and plays a crucial role in the formation of the mesoderma during vertebrate development [33], instead it seems to act by signalling through ALK4 during embryogenesis [37]. GDF11 is implicated in renal tissue and palate development and in bone marrow organogenesis when signalling through any of its receptors [31, 35]. GDF8 is a negative regulator of the growth and development of skeletal muscles [35].

Given the topological similarity of both the ligands and the receptors, we decided to investigate the structural basis of the different mode of binding of these growth factors to ALK4 and ALK7.

In more detail, we aimed at answering the following questions: what is the mode of binding of GDF3, Nodal and GDF11 to ALK7? Why is Cripto required for binding of ALK4 to GDF3 and Nodal, but not for binding of the same receptor to GDF11?

In order to answer these questions and shed some light on the intriguing question of how specificity is achieved in this complex system, we used a combination of molecular modeling and docking. We built models for the complexes between ALK7 and its three ligands (GDF3, Nodal and GDF11) and tried to rationalize the structural reasons behind the requirement for a co-factor, Cripto, in the ALK4 binding to GDF3 and Nodal.

Methods

A comparative model of the Nodal protein is available [38] while the structure of GDF8 has been determined experimentally by X-ray crystallography (PDB ID: 3HH2) [39].

Table 1 Known interactions among Transforming growth factor-beta (TGF-β) proteins of interest and their activin receptor-like kinase (ALK) receptors

ALK receptor	ALK7 (or ACVR1C)	ALK4 (or ACVR1B)
TGF-β ligand	GDF3	GDF3 (with Cripto)
	Nodal	Nodal (with Cripto)
	GDF11	GDF11
	GDF8	GDF8

Fig. 1 Ribbon representation of the BMP2/ALK3 X-ray structure (1REW) determined by Kirsch et al. [28], with BMP2 in *red* and ALK3 in *silver*. Hydrophobic residues, used as restraints in GDF3/ALK7 docking simulations, are shown as *green sticks* for BMP2 and as *orange sticks* for ALK3

We built comparative models of GDF3 (residues 251–364), GDF11 (residues 299–407) and of the extracellular domains of ALK4 (residues 24–126) and ALK7 (residues 22–113) by homology using HHpred [40, 41], which in turn uses HHSearch for identifying suitable templates and Modeller [42] for building the model. The templates used for building the comparative models of GDF3 (UniProt ID: Q9NR23) and GDF11 (UniProt ID: O95390) were BMP2 (PDB ID: 1REW; sequence identity 53%, sequence similarity 74% and coverage 66%) and GDF8 (PDB ID: 3HH2; sequence identity 90%, sequence similarity 96% and coverage 73%), respectively. The template for the ALK4 was ALK5, also called TGFBR1 (PDB ID: 2PJY; sequence identity 41%, sequence similarity 47% and coverage 72%). The same template was used to model most of the ALK7 structure (sequence identity 41%, sequence similarity 52% and sequence coverage 78%) with the exception of loop 23, where the ALK3 structure (PDB ID: 1REW; sequence identity

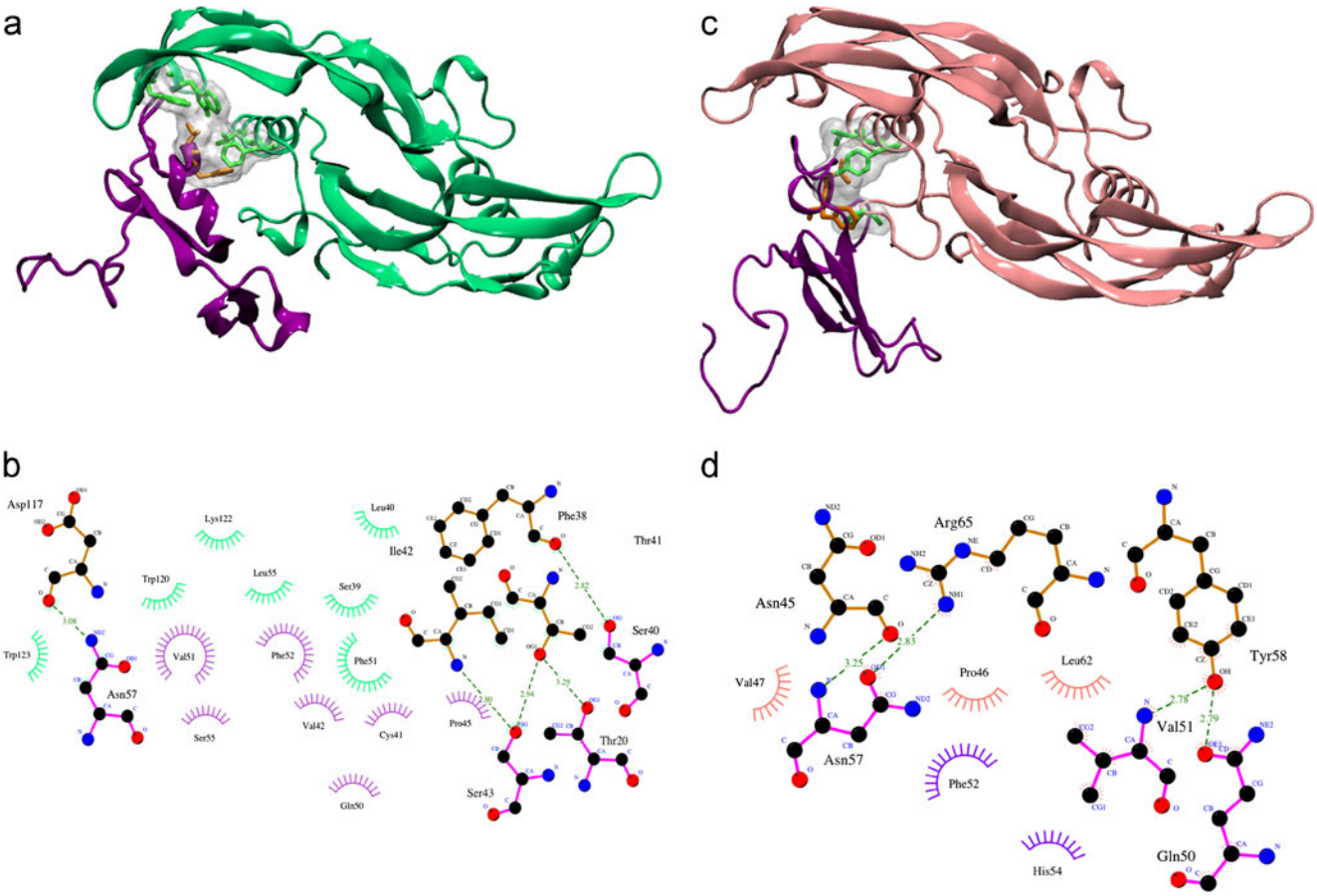

Fig. 2 Ribbon representation of the models of the **a** GDF3/ALK7 and **c** Nodal/ALK7 complexes, with GDF3 in *green*, Nodal in *pink* and ALK7 in *purple*. Hydrophobic residues at the interface are shown as *green sticks* for both ligands and as *orange sticks* for ALK7; a *light gray* Connolly surface is used to represent the knob-into-hole mode of binding. Schemes of the ligand–receptor interactions obtained by LigPlot [53] in **b** and **d**: hydrogen bonds are indicated as *dashed lines* and the residues involved are shown as *ball-and-stick models*; hydrophobic interactions are represented by *arcs* with spokes radiating towards the atoms they contact, in *green* for GDF3, in *pink* for Nodal and in *purple* for ALK7

32%, sequence similarity 31% and coverage 85%) was used. ALK3 is also known by the alternative name BMPR1A. The sequence alignments between the target and the templates are shown in the Supplementary Material Fig. S2. Model quality was assessed visually and using the QMEAN server [43, 44].

The complex between ALK7 and GDF3 was built initially using a template-based approach, based on the structure of the BMP2/ALK3 complex. The main chain atoms of the GDF3 and ALK7 comparative models were optimally superimposed with the main chains of BMP2 and ALK3 in the complex. Residues in the BMP2/ALK3 interface that were also conserved in the GDF3/ALK7 interface were used subsequently as restraints in a docking experiment with HADDOCK [45] using explicit solvent.

The same strategy was used to build the Nodal/ALK7 complex using the TGF-β/ALK homologous complex as initial template.

The modeling of the GDF11/ALK7, GDF8/ALK7, GDF11/ALK4 and GDF8/ALK4 complexes could not take advantage of the availability of a homologous complex. Although GDF11 is similar to GDF8, which indeed we used as template, the only known complex of the latter includes an antagonist, Follistatin, and not a type I receptor.

The models were therefore obtained using ClusPro [46, 47] with default parameters and subjected to a refinement in explicit solvent using HADDOCK.

All the modeled complexes were analyzed with the PIC web server [48] to identify the ligand–receptor interactions. Relevant residues for binding were analyzed performing an in silico alanine scanning as implemented in DrugScorePPI [49, 50] and Robetta [51]. In both methods, residues with a $\Delta\Delta G$ larger than 1,0 kcal mol^{-1} are predicted to be essential for the interaction. A different tool, HotPoint [52], based on the extent of buried accessible surface area upon complex formation (relΔASA) and pair potentials, was also used. A relΔASA larger than 20.0 Å and a pair potential above 18.0 $Jmol^{-1}$ indicates that the residue is likely to contribute significantly to the binding energy.

Table 2 Summary of the interactions observed in complexes involving ALK7

Complex	GDF3	ALK7	Nodal	ALK7	GDF11	ALK7	GDF8	ALK7
Hydrophobic interactions	Pro38	Leu10	Pro46	Trp25	Leu4	Leu10	Leu4	Leu10
	Ile42	Pro45	Trp134	Ala59	Met52		Val50	Trp25
	Phe51	Val51	Pro46	Val51	Met50	Trp25	Phe2	
	Leu55		Tyr58		Phe51		Phe51	Met29
	Trp120		Leu62		Tyr49	Met29	Phe51	Ile38
	Trp123		Pro46	Phe52	Phe51		Leu52	
	Phe38	Phe52	Val47		Phe51	Ile38	Ile141	Ala49
	Phe51		Tyr58		Ile141	Ala49	Trp138	
	Ala54				Met193		Trp140	
	Leu55				Tyr195		Pro56	Val51
					Pro56	Val51	Leu60	
					Trp138		Trp138	
					Met50	Phe52	Met210	
					Pro56		Val50	Phe52
							Pro56	
Hydrogen bonds	Thr20	Phe38	Tyr58	Gln50	Tyr49	His54	Tyr195	Leu47
	Ser43	Thr41	Arg65	Val51	Gln62	Ser55	Phe136	His54
	Asn57	Asp117	Asn45	Asn57	Gln63	Asn56	Gln63	Ser55
					Phe136	Asn57	His62	Asn57
							Arg14	Met29
							Glu12	Gln36
							Met210	Asn48
							Glu48	Asn58
Ionic interactions					Lys54	Glu46		
Aromatic-sulfur interactions					Met50	Phe52		
Cation-π interactions					Lys54	Phe52		
Aromatic-aromatic					Phe51	Trp25	Phe2	Trp25

Results and discussion

The model of the GDF3/ALK7 complex, obtained as described in Methods, was built using the BMP2/ALK3 complex as template. Residues in the BMP2/ALK3 interface (Fig. 1), conserved in the GDF3/ALK7 interface, were used as restraints in a docking experiment with HADDOCK [45]. The model of the GDF3/ALK7 complex is shown in Fig. 2a, b.

Residues used as constraints in the docking simulation were Val51 of ALK7 and Pro 50, Phe51 and Leu55 of GDF3. The final model achieved a QMEAN score of 0.49 and a QMEAN Z-score of −2.96. By analyzing the complex using DrugScorePPI, Robetta and HotPoint, the same residues were identified as important for complex stability, namely those belonging to the "wrist epitope" of GDF3 and Val51 and Phe52 of ALK7. Most of the interactions are hydrophobic or mediated by hydrogen bonds (Table 2).

Val 51 of ALK7 is situated in a hydrophobic pocket of GDF3 formed by Phe 51 and Leu 55 (belonging to the α3 of the GDF3 monomer) and Trp 120 and Trp 123 (belonging to the other GDF3 monomer) (Fig. 2a). Our model of the complex structure shows a knob-into-hole packing mechanism as proposed by Kirsch et al. [28] for the homologous BMP2/ALK3 complex determined experimentally. In this latter complex, Phe 85 in the α1 helix of ALK3 (corresponding to Val 51 in ALK7) interacts with hydrophobic residues in the BMP2 "wrist epitope" (a region similar to the corresponding one in GDF3).

A similar mode of interaction is observed in the modeled Nodal/ALK7 complex (QMEAN score and QMEAN Z-score equal to 0.50 and −2.81, respectively) shown in Fig. 2c,d with one important difference. Critical residues for the interaction, identified as described in Methods, are those belonging to helix α3 of one Nodal monomer (specifically Pro 46, Tyr 58 and Leu 62) and to loop 23 of the ALK7 (Val 51) (Fig. 2c). This means that, at variance from what we observed in the GDF3/ALK7, in this case the binding interactions involve only one Nodal monomer. The interactions observed in the TGF-β complexes with ALK7 are shown in Table 2.

In the GDF11/ALK7 complex (QMEAN score and QMEAN Z-score equal to 0.42 and −3.66, respectively), shown in Fig. 3, the GDF11 residues around the "wrist epitope", in particular in the pre-helix loop of one monomer and in the loop between sheet β2 and β3 of the other, form the core of the interaction. Interestingly, the interface between ALK7 and GDF11 is more extended than what we observed in the complexes of the same receptor with its Nodal and GDF3 ligands. The buried surface area (BSA) for GDF11/ALK7 complex is equal to 2,102 Å^2, while for Nodal/ALK7 and GDF3/ALK7 it is 1,700 Å^2 and 1,682 Å^2, respectively.

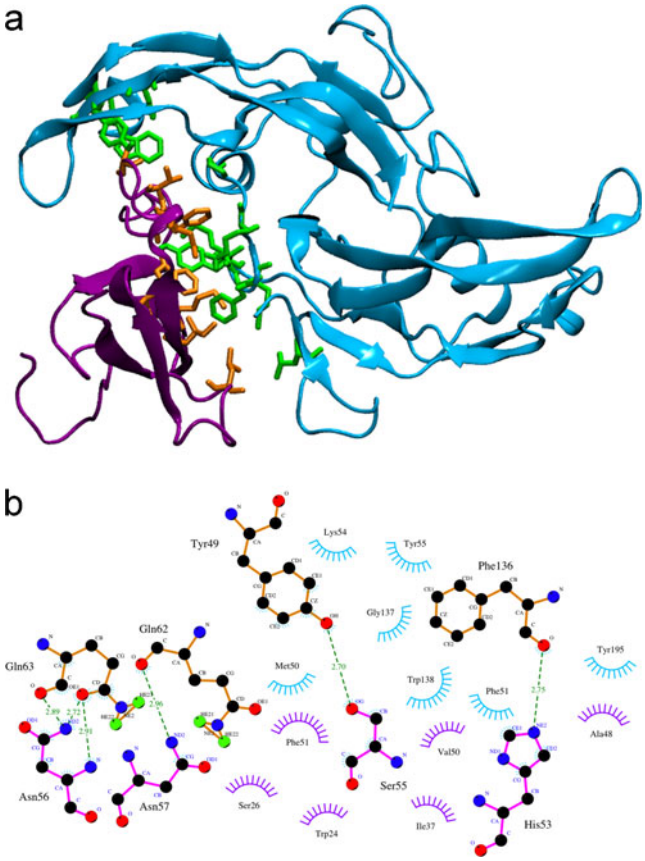

Fig. 3 **a** Ribbon representation of the model of the GDF11/ALK7 complex, with GDF11 in *cyan* and ALK7 in *purple*. Hydrophobic residues at the interface are shown as *green sticks* for GDF11 and as *orange sticks* for ALK7. **b** Scheme of ligand–receptor interactions obtained by LigPlot [53]: residues involved in hydrophobic interactions are represented in *cyan* for GDF11 and in *purple* for ALK7. Symbols as in Fig. 2

The GDF8/ALK7 complex (QMEAN score of 0.47 and QMEAN Z-score of −3.20) shows a binding interface similar to that observed in the GDF11/ALK7 complex, with a BSA of 2,520 Å^2 (data not shown). The ALK7 receptor occupies the whole GDF8 binding site, and the core of interaction is formed by residues on the "wrist epitope" for GDF8 and by the region including loop 23 of the receptor (Table 2).

The models of the ALK4 in complex with GDF11 and GDF8 (Fig. 4) also share some common properties (QMEAN scores equal to 0.46 and 0.47 and QMEAN Z-scores equal to −3.28 and −3.17 for GDF11/ALK4 and GDF8/ALK4, respectively). The amino acids important for the interaction are mostly hydrophobic and located in the "wrist epitope" and on the N-terminal region of the ligands and span the entire region that includes loop 23 of the receptor. The interactions involved in the complexes with ALK4 are summarized in Table 3. Interestingly, our docking procedure produced a reasonable hypothesis for the formation of all the complexes of ALK7 and for those involving ALK4 and GDF11 and GDF8, but no solution could be found when we attempted to dock the GDF3 and Nodal structures and their ALK4 receptor.

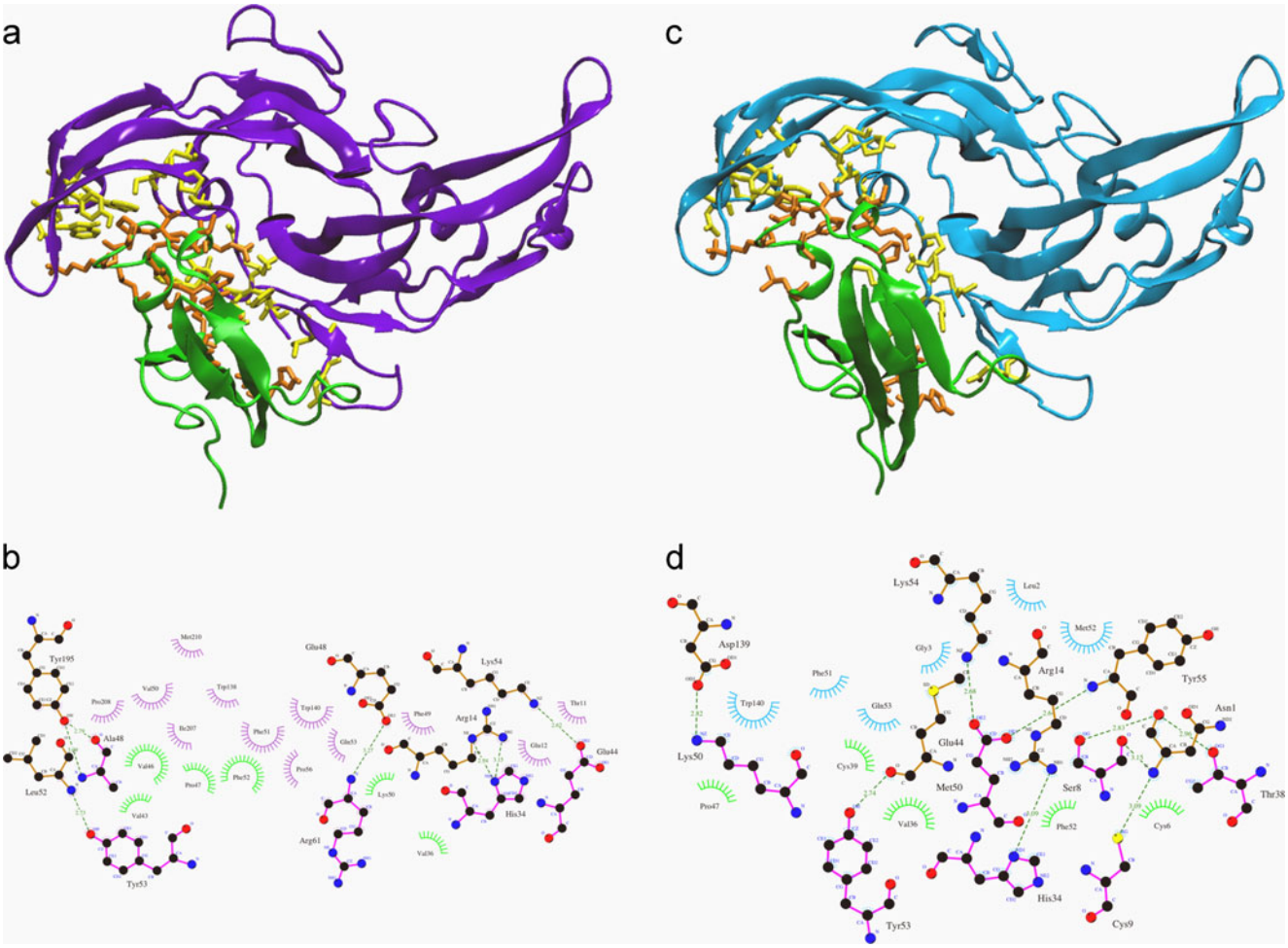

Fig. 4 Ribbon representation of the models of the **a** GDF8/ALK4 and **c** GDF11/ALK4 complexes, with GDF8 in *purple*, GDF11 in *cyan* and ALK4 in *green*. Hydrophobic residues at the interface are shown as *yellow sticks* for both ligands and as *orange sticks* for ALK4. **b**, **d** Schemes of ligand–receptor interactions obtained by LigPlot [53]; residues involved in hydrophobic interactions are colored *cyan* for GDF11, in *purple* for GDF8 and in *green* for ALK4. Symbols as in Fig. 2

This is obviously interesting, since it is known that the Cripto co-factor is required in these two cases [32, 33]. The following question arises: what are the structural reasons why it seems impossible to form this complex?

We superimposed the GDF3 and Nodal models to the GDF11 in complex with ALK4. The result shows that the main determinant for the different mode of interaction is very likely to be the pre-helix loop of the ligands (Fig. 5). This loop, which is important for the formation of all complexes examined, is two residues longer in GDF3 and Nodal (Fig. 6). This would lead to a steric hindrance between the receptor and these two ligands if they had to assume the same relative position as GDF11 and GDF8 in the complex with ALK4. Therefore, GDF3 and Nodal are unlikely to bind directly to the ALK4 receptor, in agreement with experimental data showing that the Cripto co-factor is required to mediate their binding [32, 33].

To investigate the reason why GDF3 and Nodal can instead bind ALK7 in a fashion similar to binding of GDF11 and GDF8, we superimposed ALK4 on ALK7 in complex with GDF3 and Nodal. In this case, the shorter length of loop 23 in ALK7 is the key determinant. In fact, the ALK4 loop 23 would occupy the same portion of space as the pre-helix loop of the GDF3 and Nodal ligands if they formed a complex similar to that formed with ALK7.

Summary

The combination of homology modeling and docking experiments is a powerful tool for investigating interactions among proteins that are not sufficiently well characterized and might lead to interesting hypotheses that can be tested experimentally.

Here we show that a rather complex system, composed of two receptors and four ligands with fine-tuned specificity, can be analyzed computationally and that the results can be used effectively to design appropriate experiments.

Table 3 Summary of the interactions observed in the complexes involving ALK4

Complex	GDF11	ALK4	GDF8	ALK4
Hydrophobic interactions	Leu2	Pro41	Phe2	Ile40
	Met50	Phe52		Pro41
		Tyr53	Leu4	Val36
	Phe51	Phe27	Phe49	Leu55
		Val36	Val50	Phe52
	Met52	Val36		Tyr53
	Pro56	Val46	Leu52	Met23
		Phe52	Pro56	Val36
	Leu60	Phe52	Trp138	Val46
	Trp138	Val46		Phe52
		Pro47		Val46
		Phe52	Trp140	Pro47
	Trp140	Pro47	Ile141	Phe52
		Phe52	Tyr195	Pro47
		Leu55		Pro47
	Ile141	Pro47		Pro47
	Met193	Val46		Ala48
	Tyr195	Pro47	Ile207	Val46
		Ala48		Pro47
	Ile207	Val43	Pro208	Val43
		Val46		Val46
	Pro208	Val43	Met210	Val46
	Met210	Val46		
Hydrogen bonds	Asn1	Cys9	Arg14	His34
	Ser8	His34	Gly48	Glu44
	Arg14	Met50	Lys54	Tyr53
	Gln14	Tyr53	Tyr195	Arg61
	Lys54	Lys54		
	Tyr55			
	Asp139			
Ionic interactions	Glu12	His34	Glu12	His34
	Lys54	Glu44	Glu48	His35
	Asp139	Lys50	Lys54	Glu44
			Asp139	Arg61
				Lys50
Aromatic-sulfur interactions	Met50	Phe52		
		Tyr53		
Cation-π interactions	Tyr49	Arg61	Arg14	Phe27
	Lys54	Tyr53	Trp140	Lys50
	Trp140	Lys50		
Aromatic-aromatic	Phe51	Phe27	Phe51	Tyr53
	Trp138	Phe52		

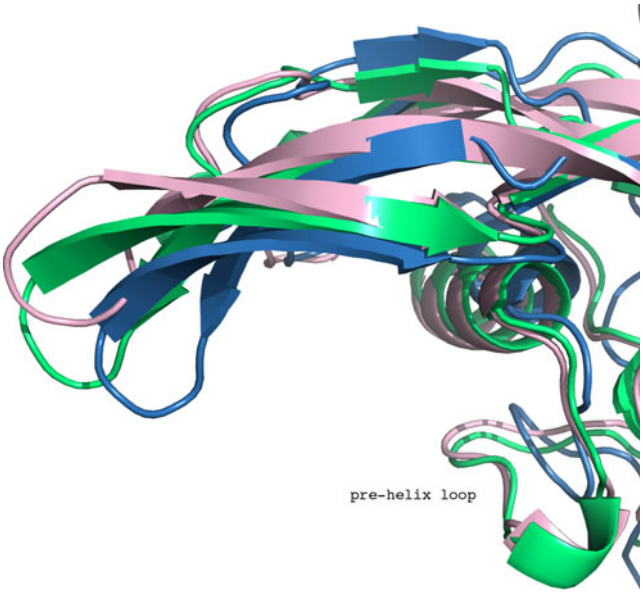

Fig. 6 Superposition of the pre-helix loops of GDF3 (in *light green*), Nodal (in *pink*) and GDF11 (in *blue*)

In the absence of experimental structures for the TGF-β/ALK complexes studied here, the availability of computational models, obtained by homology and protein-protein docking simulations, allows the analysis of the putative binding interfaces and the identification of structural features and specific elements deemed to be crucial for selective binding.

In particular, in the TGF-β (Nodal, GDF3, GDF11) complexes with ALK7, binding is essentially driven by hydrophobic interactions. On the other hand, the TGF-β (GDF8, GDF11) complexes with ALK4 show a binding mode characterized by hydrophobic and ionic interactions as well.

Furthermore, our results suggest that the inability of GDF3 and Nodal to bind ALK4 directly is likely due to the steric hindrance caused by the length of both the TGF-β pre-helix loops and the ALK4 loop 23.

Our data provide a structural explanation for the requirement of the Cripto co-factor in the formation of the GDF3/ALK4 and Nodal/ALK4 complexes since our models show that the ligands cannot bind the receptor in the canonical

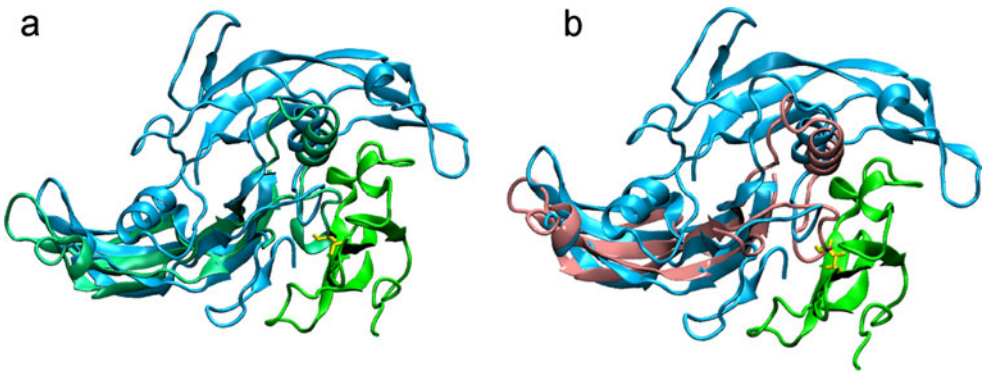

Fig. 5 Superposition of **a** the GDF3 monomer (in *light green*) and **b** the Nodal monomer (in *pink*) to GDF11 (in *cyan*) in complex with the ALK4 receptor (in *green*). In both figures, only the GDF3 and Nodal monomers are shown for clarity and two residues (E49 for Nodal and T41 for GDF3) of the pre-helix loop are shown in *yellow stick* representation to orient the reader

fashion observed in all complexes where the co-factor is not required.

Our hypotheses can be verified experimentally by performing binding assays with peptide sequences designed ad hoc to mimic the potential binding epitopes; such experiments are in progress.

Acknowledgments King Abdullah University of Science and Technology (KAUST; Award No. KUK-I1-012-43); Fondazione Roma and the Italian Ministry of Health (contract no.onc_ord 25/07, FIRB ITALBIONET and PROTEOMICA).

Ministero dell'Università e della Ricerca Scientifica (MIUR), project PRIN n° prot. 2008F5A3AF_001.

References

1. Lin SJ, Lerch TF, Cook RW, Jardetzky TS, Woodruff TK (2006) The structural basis of TGF-beta, bone morphogenetic protein, and activin ligand binding. Reproduction 132:179–190
2. Shi Y, Massague J (2003) Mechanisms of TGF-beta signaling from cell membrane to the nucleus. Cell 113:685–700
3. Chang H, Brown CW, Matzuk MM (2002) Genetic analysis of the mammalian transforming growth factor-beta superfamily. Endocr Rev 23:787–823
4. Kingsley DM (1994) The TGF-beta superfamily: new members, new receptors, and new genetic tests of function in different organisms. Genes Dev 8:133–146
5. Bierie B, Moses HL (2006) Tumour microenvironment: TGFbeta: the molecular Jekyll and Hyde of cancer. Nat Rev Cancer 6:506–520. doi:10.1038/nrc1926
6. Pardali K, Moustakas A (2007) Actions of TGF-beta as tumor suppressor and pro-metastatic factor in human cancer. Biochim Biophys Acta 1775:21–62. doi:10.1016/j.bbcan.2006.06.004
7. Munir S, Xu G, Wu Y, Yang B, Lala PK, Peng C (2004) Nodal and ALK7 inhibit proliferation and induce apoptosis in human trophoblast cells. J Biol Chem 279:31277–31286
8. Li MO, Flavell RA (2008) TGF-beta: a master of all T cell trades. Cell 134:392–404. doi:10.1016/j.cell.2008.07.025
9. Watabe T, Miyazono K (2009) Roles of TGF-beta family signaling in stem cell renewal and differentiation. Cell Res 19(1):103–115. doi:10.1038/cr.2008.323
10. Dennler S, Goumans MJ, ten Dijke P (2002) Transforming growth factor beta signal transduction. J Leukoc Biol 71:731–740
11. Rosbottom A, Scudamore CL, von der Mark H, Thornton EM, Wright SH, Miller HR (2002) TGF-beta 1 regulates adhesion of mucosal mast cell homologues to laminin-1 through expression of integrin alpha 7. J Immunol 169:5689–5695
12. Kandasamy M, Reilmann R, Winkler J, Bogdahn U, Aigner L (2011) Transforming growth factor-beta signaling in the neural stem cell niche: a therapeutic target for Huntington's disease. Neurol Res Int 2011:124256. doi:10.1155/2011/124256
13. Krieglstein K, Strelau J, Schober A, Sullivan A, Unsicker K (2002) TGF-beta and the regulation of neuron survival and death. J Physiol Paris 96:25–30
14. Hogan BL (1996) Bone morphogenetic proteins: multifunctional regulators of vertebrate development. Genes Dev 10:1580–1594
15. Massague J (2008) TGFbeta in Cancer. Cell 134:215–230. doi:10.1016/j.cell.2008.07.001
16. Padua D, Massague J (2009) Roles of TGFbeta in metastasis. Cell Res 19:89–102. doi:10.1038/cr.2008.316
17. Goumans MJ, Liu Z, ten Dijke P (2009) TGF-beta signaling in vascular biology and dysfunction. Cell Res 19:116–127. doi:10.1038/cr.2008.326
18. Blobe GC, Schiemann WP, Lodish HF (2000) Role of transforming growth factor beta in human disease. N Engl J Med 342 (18):1350–1358. doi:10.1056/NEJM200005043421807
19. de Caestecker M (2004) The transforming growth factor-beta superfamily of receptors. Cytokine Growth Factor Rev 15:1–11
20. Barbault F, Landon C, Guenneugues M, Meyer JP, Schott V, Dimarcq JL, Vovelle F (2003) Solution structure of Alo-3: a new knottin-type antifungal peptide from the insect *Acrocinus longimanus*. Biochemistry 42:14434–14442. doi:10.1021/bi035400o
21. McDonald NQ, Lapatto R, Murray-Rust J, Gunning J, Wlodawer A, Blundell TL (1991) New protein fold revealed by a 2.3-A resolution crystal structure of nerve growth factor. Nature 354:411–414. doi:10.1038/354411a0
22. Vitt UA, Hsu SY, Hsueh AJ (2001) Evolution and classification of cystine knot-containing hormones and related extracellular signaling molecules. Mol Endocrinol 15:681–694
23. Manning G, Whyte DB, Martinez R, Hunter T, Sudarsanam S (2002) The protein kinase complement of the human genome. Science 298:1912–1934
24. Greenwald J, Fischer WH, Vale WW, Choe S (1999) Three-finger toxin fold for the extracellular ligand-binding domain of the type II activin receptor serine kinase. Nat Struct Biol 6:18–22
25. Thompson TB, Woodruff TK, Jardetzky TS (2003) Structures of an ActRIIB:activin A complex reveal a novel binding mode for TGF-beta ligand:receptor interactions. EMBO J 22:1555–1566
26. Sieber C, Kopf J, Hiepen C, Knaus P (2009) Recent advances in BMP receptor signaling. Cytokine Growth Factor Rev 20:343–355
27. Allendorph GP, Vale WW, Choe S (2006) Structure of the ternary signaling complex of a TGF-beta superfamily member. Proc Natl Acad Sci USA 103:7643–7648
28. Kirsch T, Sebald W, Dreyer MK (2000) Crystal structure of the BMP-2-BRIA ectodomain complex. Nat Struct Biol 7:492–496
29. Santibanez JF, Quintanilla M, Bernabeu C (2011) TGF-beta/TGF-beta receptor system and its role in physiological and pathological conditions. Clin Sci (Lond) 121:233–251
30. Andersson O, Korach-Andre M, Reissmann E, Ibanez CF, Bertolino P (2008) Growth/differentiation factor 3 signals through ALK7 and regulates accumulation of adipose tissue and diet-induced obesity. Proc Natl Acad Sci USA 105:7252–7256
31. Andersson O, Reissmann E, Ibanez CF (2006) Growth differentiation factor 11 signals through the transforming growth factor-beta receptor ALK5 to regionalize the anterior-posterior axis. EMBO Rep 7:831–837
32. Chen C, Ware SM, Sato A, Houston-Hawkins DE, Habas R, Matzuk MM, Shen MM, Brown CW (2006) The Vg1-related protein Gdf3 acts in a Nodal signaling pathway in the pre-gastrulation mouse embryo. Development 133:319–329
33. Reissmann E, Jornvall H, Blokzijl A, Andersson O, Chang C, Minchiotti G, Persico MG, Ibanez CF, Brivanlou AH (2001) The orphan receptor ALK7 and the Activin receptor ALK4 mediate signaling by Nodal proteins during vertebrate development. Genes Dev 15:2010–2022
34. Walpole IR, Grauaug A (1979) Intra-uterine infection with herpes simplex virus and observed radiological changes. Aust Paediatr J 15:123–125
35. Tsuchida K, Nakatani M, Uezumi A, Murakami T, Cui X (2008) Signal transduction pathway through activin receptors as a therapeutic target of musculoskeletal diseases and cancer. Endocr J 55:11–21
36. Levine AJ, Brivanlou AH (2006) GDF3, a BMP inhibitor, regulates cell fate in stem cells and early embryos. Development 133:209–216
37. Schier AF, Shen MM (2000) Nodal signalling in vertebrate development. Nature 403:385–389

38. Calvanese L, Marasco D, Doti N, Saporito A, D'Auria G, Paolillo L, Ruvo M, Falcigno L (2010) Structural investigations on the Nodal-Cripto binding: a theoretical and experimental approach. Biopolymers 93:1011–1021
39. Cash JN, Rejon CA, McPherron AC, Bernard DJ, Thompson TB (2009) The structure of myostatin:follistatin 288: insights into receptor utilization and heparin binding. EMBO J 28:2662–2676
40. Soding J (2005) Protein homology detection by HMM–HMM comparison. Bioinformatics 21:951–960
41. Soding J, Biegert A, Lupas AN (2005) The HHpred interactive server for protein homology detection and structure prediction. Nucleic Acids Res 33 (Web Server issue):W244–W248
42. Fiser A, Sali A (2003) Modeller: generation and refinement of homology-based protein structure models. Methods Enzymol 374:461–491
43. Baker D, Sali A (2001) Protein structure prediction and structural genomics. Science 294:93–96
44. Benkert P, Tosatto SC, Schomburg D (2008) QMEAN: A comprehensive scoring function for model quality assessment. Proteins 71:261–277
45. de Vries SJ, van Dijk M, Bonvin AM (2010) The HADDOCK web server for data-driven biomolecular docking. Nat Protoc 5:883–897
46. Comeau SR, Gatchell DW, Vajda S, Camacho CJ (2004) ClusPro: an automated docking and discrimination method for the prediction of protein complexes. Bioinformatics 20:45–50
47. Kozakov D, Brenke R, Comeau SR, Vajda S (2006) PIPER: an FFT-based protein docking program with pairwise potentials. Proteins 65:392–406
48. Tina KG, Bhadra R, Srinivasan N (2007) PIC: Protein Interactions Calculator. Nucleic Acids Res 35 (Web Server issue):W473–W476
49. Gohlke H, Hendlich M, Klebe G (2000) Knowledge-based scoring function to predict protein-ligand interactions. J Mol Biol 295: 337–356
50. Kruger DM, Gohlke H DrugScorePPI webserver: fast and accurate in silico alanine scanning for scoring protein-protein interactions. Nucleic Acids Res 38 (Web Server issue):W480–W486
51. Kortemme T, Kim DE, Baker D (2004) Computational alanine scanning of protein–protein interfaces. Sci STKE 2004 (219):pl2
52. Tuncbag N, Gursoy A, Keskin O (2009) Identification of computational hot spots in protein interfaces: combining solvent accessibility and inter-residue potentials improves the accuracy. Bioinformatics 25:1513–1520
53. Wallace AC, Laskowski RA, Thornton JM (1995) LIGPLOT: a program to generate schematic diagrams of protein-ligand interactions. Protein Eng 8:127–134